

Development and Integration of Inkjet-Printed Strain Sensors for Angle Measurement of an Origami-Based Delta Mechanism

Merve Acer Kalafat 

Istanbul Technical University, Department of Mechanical Engineering, Istanbul, Turkey

ABSTRACT

An origami-based parallel mechanism is an excellent solution for various applications where small-scale, low profile, and foldability are needed. These mechanisms are composed of rigid and flexible layers designed according to layer-by-layer fabrication methods. In addition, it becomes important to design functional layers that provide user feedback. Here, the design and fabrication of an origami-based 3 Degree-of-Freedom (DoF) Delta mechanism, which has the same traditional kinematics as a Delta mechanism, are presented. A sensor layer was designed composed of 3 strain gauges to measure the angular position of the actuated arm of the mechanism. The strain-gauge patterns were printed on a special Polyethylene terephthalate (PET) using Silver nanoparticle ink with a commercial desktop printer. The integration of these sensors has been studied by placing them in different locations between rigid layers. The sensors' outputs were presented when subjected to step and sinusoidal inputs of the actuated arm. The experiment results show that the developed sensor layer can track the angular position changes of the actuated lower arm, which is a promising result to be used in a control loop in the future.

Keywords:

Origami-based mechanisms; Foldable mechanisms; Parallel platforms; Delta mechanism; Soft robots; Inkjet printed sensors; Strain sensors

Article History:

Received: 2022/10/17

Accepted: 2022/12/05

Online: 2022/12/31

Correspondence to: Merve Acer Kalafat,
Istanbul Technical University, Department
of Mechanical Engineering, Istanbul,
Turkey
E-mail: acerm@itu.edu.tr;
Phone: +90 0212 293 1300 – 2471

INTRODUCTION

Today, robotic systems are not only desired to be large-scale mechanical structures designed for a single task used only in industrial applications but also needed to perform tasks in medicine, defense, space, and service applications. Besides, they start to take more place in our daily lives. With the increase in the diversity in the field of application, it has become necessary to develop and produce robotic systems at different scales and using different materials, as well as to adapt to different working conditions. Parallel mechanisms have been preferred due to their low inertia, high precision, rigidity, and sensitivity, despite their limited working space, complex structure, and direct kinematic modeling that is difficult to solve [1], [2]. They are used in various fields, such as motion simulation in large dimensions, pick-and-place operations, welding and processing, food packaging, 3D printers, etc. Their existing advantages can be increased significantly by the miniaturization of large-scale parallel mechanisms. One of the most popular parallel mechanisms is the “Delta” mechanism.

It was developed by Clavel with 3 DoF to perform a pick-and-place process in a food production facility [3]. Delta robot ensures that the orientation and translation movements of the moving platform are performed independently of each other. It is advantageous in terms of high rigidity and speed. Besides, it is easy to find a closed kinematic solution. For this reason, Delta robots are widely used in the food, medical, pharmaceutical, and electronics industries [1]. In addition, medium and small-sized Delta robots have begun to be used in applications that require high precision, such as cell manipulation, micro-manufacturing/micro-assembly, and micro-surgery [4], [5], [6].

Conventional machine elements (such as gears, wheels, screws, nuts, and profiles) and materials (such as steel and aluminum) used in industrial and large-sized robotic systems are almost impossible for miniature robotic systems in cm and below. Therefore, monolithic fabrication techniques have started to develop. These techniques replace traditional fabrication methods with

a characteristic size of cm or less, enabling efficient mass production while eliminating components' troublesome assembly and assembly processes [7]. In addition, high-performance, durable, complex, articulated structures and systems are produced cheaply, quickly, and scalable [8]. One of the popular robotic designs suitable for monolithic fabrication techniques is origami-based designs. It is the ability to create three-dimensional (3D) structures using two-dimensional (2D) materials. It is based on the principle of forming a single composite structure by the layer-by-layer composition of different layers of materials [7]. The materials can be chosen as metal or polymer according to the mechanism's structural features. The origami-based monolithic fabrication method is a technology that is still being developed. In the literature, there are mobile origami-based robots that mimic insects in nature [9], [10], [11], [12]. In addition, due to this method's high potential in producing fast, inexpensive, durable robotic systems, endoscopic medical devices have started to be designed using this method [13], [14].

This work presents a novel origami-based, sensor-integrated Delta mechanism. And in the literature, there are also origami-based parallel platforms. Salerno et al. [15] implemented a collapsible parallel platform design and integrated a single-degree-of-freedom electromagnetic actuator into the mechanism. Temel et al. [16] produced another foldable new Delta mechanism called milliDelta. Mintchev et al. [17] have designed a new 3 DoF parallel mechanism that can be used for human-robot interaction, which was also carried out. However, these mechanisms need manual-folding and chemical or mechanical bonding processes in their fabrication. Kalafat Acer et al. [18] developed a novel Delta mechanism having a new parallelogram joint design that eliminates extra bonding processes, providing monolithic top to bottom during the assembly.

As the dimensions of the robotic systems get smaller, it has become necessary to reduce the size of the robotic components such as actuators, sensors, and controllers. Besides, it is important to design them with a completely innovative perspective to integrate them into the robotic systems manufactured with the monolithic production method. Origami-based robots need embedded sensors to provide feedback for their motion control. Commercial sensors are not customizable and scalable. Therefore, novel sheet-type sensors are being studied that can be integrated into mechanisms. Recently, new ink and printing technologies have been developed, along with technologies such as RFID tags, wearable electronics, and degradable biomedical devices. Inkjet and screen printing methods are used for foldable robots based on printing specified patterns using conductive inks onto sheets. The screen printing method is widely used in flexible sensor manufacturing. It can be compatible with

various inks, from polymers to metals. Besides, it is widely used in wearable electronics for resistive and capacitive type sensors. Firouzeh et al. [19], for the first time in the literature, designed and manufactured an origami robot called "Robogami," which incorporates all the actuator, sensor, and control layers into the laminated structure. They have used the screen printing technique for their piezoresistive sensor based on carbon ink. Kwak et al. [20] used the electrical contact resistance change to detect the bending angle of a foldable laminated mechanism flexible joint. They used a screen printing technique with conductive polymer ink PEDOT:PSS to create two opposing conductive fields on flexible substrates. However, screen printing has some disadvantages, such as material waste, mold requirement, low pattern resolution, and high minimum printing thickness. Therefore, inkjet printed sensors became popular because they don't require a mold, provide high resolution and low profile, have much lower material waste, and are easier to customize [21, 22]. Sun et al. [23] used a desktop commercial printer and developed a sensor using carbon ink. The sensor layer is embedded in the laminated structure with one end fixed and the other end slider. Thus the sensor moves freely in its housing when the joint is bent. Vadgama et al. [24] produced high reproducibility sensors for prototypes of different scales by printing silver nanoparticle ink on PET substrates with an inkjet printer. However, the lowest working radius of curvature is 30 mm scales which corresponds to relatively very low strain values for curvature detectors. For foldable origami-based cm scale parallel mechanisms, much smaller radii of curvature (1 mm) are needed. Ando et al. [25] have also used Silver Nanoparticle (Ag NP) ink printing on a PET substrate with an office-type inkjet printer. They have also used a strain-gauge pattern. But they have not embedded the sensor in a foldable structure.

In this work, sensor integration to an origami-based Delta mechanism is studied. The mechanism is our novel design which is presented in [18]. Here, sensor integration into the developed Delta mechanism is the main contribution. The strain gauge sensors are printed using Ag NP ink with a commercial desktop printer. These sensors are developed as a flexible layer that can be embedded in the layers of the mechanism. It has been observed that the placement of the sensors affects the tracking of the active joint angles. Therefore, the joint angle tracking performance has been analyzed for three different placements. And it has been shown that the results are promising for providing joint angle feedback to a closed-control loop.

This paper is organized as follows: in the Materials and Methods section, the design and fabrication of the mechanism, the fabrication and integration of the sensor, and finally, the used experimental setup are presented. Then, in the Results and Discussion section, the sensors' output sig-

nals were analyzed with different joint angle inputs. Lastly, in the Conclusion section, the paper is concluded.

MATERIAL AND METHODS

Design and Fabrication of the Mechanism

In the Delta mechanism, three kinematic chains connect the movable platform to the stationary base platform [3]. These kinematic chains consist of two branches; the upper link is connected to the movable platform, and the lower link is connected to the fixed lower platform. There is a 1 DoF revolute joint between the lower link and the base platform. With this joint, the opposite side of the lower link will always be parallel to the lower platform, making the connection between the upper and lower links parallel. The upper link must be a parallelogram to maintain this parallel movement between platforms. A parallelogram keeps its opposing links parallel, which then parallels the movement of the mobile platform to the base platform. The mechanism requires universal joints at the parallelograms, which challenges using only 2D fabrication methods. In the literature, there are Delta mechanism designs inspired by origami [16], [26]. But all of them need an assembly process (often called out-of-plane folding) where they must fold the link or glue other materials to achieve the desired mechanism. The challenge is to design the structure with a purely on-plane design method. Here presented design uses novel 2 DoF joints (initially flat and in the same plane) that can operate in 3D space, as shown in Fig 1c. Detailed information can be found in [18].

The designed Delta mechanism has the base and moving platform layers, as shown in Fig. 1a. The Base platform layer has 1 DoF simple active revolute joints for the lower arms, which are actuated with servo motors. The moving platform has parallelograms that enable the connection between the base and moving platforms (Fig. 1b).

Traditional Delta mechanism's kinematic model [1], [3] was used to design the origami-based mechanism. The geo-

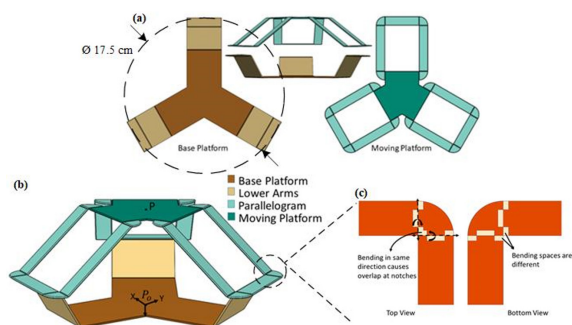


Figure 1. Origami-based Delta mechanism design: (a) Flat base and moving platforms consisting of joints and arms, (b) Assembled Delta mechanism, (c) Novel 2D joint designs on the parallelogram.

metric parameters of the mechanism were selected in such a way that it can perform its task in a 20x20x20 mm³ cubic space. It has a 17.5 cm circular footprint when it is entirely flat (Fig. 1a). However, the designed Delta mechanism has different connection types from the traditional one. This difference is mainly due to the connection points created for 2D manufacturing methods. Since the designed Delta mechanism's parallelogram arms have 2 DoF joints that mimic true universal connections (Fig. 1c). One closed kinematic chain of the developed Delta mechanism is presented in Fig 2a. The base platform is fixed, and the lower arm is actuated using a motor. The designed parallelogram, the upper arm, and the connected moving platform are moving according to the given θ_i input. The center of the moving platform presented as P has the trajectory of a sphere for one kinematic closed-loop chain. Detailed information about origami-based design and the kinematics of the Delta mechanism can be found in [18].

The parallelogram structure was analyzed to determine whether it maintains parallel motion throughout the mechanism's motion. Therefore, a 3D CAD model of the mechanism was developed. The lower arms were actuated with the same motion profile using the kinematics and CAD models. The results were compared to see if the mathematical model is the same as the CAD model, which is the ideal representation of the fabricated Delta mechanism. One arm starting from 30° had a sinusoidal motion of $\pm 15^\circ$ with a frequency of 0.5 Hz in the 0° direction. The other arm starting at 30° had a sinusoidal motion of $\pm 22.5^\circ$ in the 90° direction with a frequency of 0.25 Hz. The last arm was fixed at 45° . The results of the motion of the moving platform in the X, Y, and Z axes using the analytical kinematic and CAD models are presented in Fig 2b.

As shown in Fig. 2b, both models have consistent results. However, there are errors on a scale of 10^{-4} because the CAD model equation solver has numerical computation; the mathematical model can be said to be analytical and precise. As a result, it can be said that the kinematic equation of the traditional Delta mechanism can be used to control and analyze the origami-based Delta mechanism.

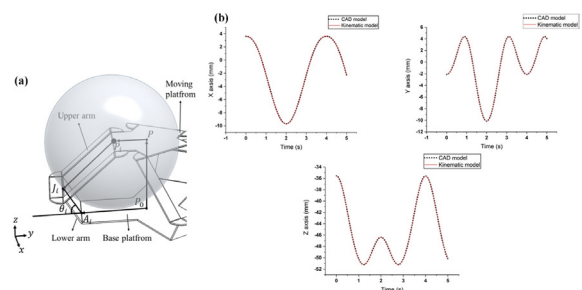


Figure 2. (a) One kinematic closed-loop chain of the Delta mechanism, (b) Kinematics and CAD models comparison test results: moving platform's center motion on the X-axis, Y-axis, and Z-axis.

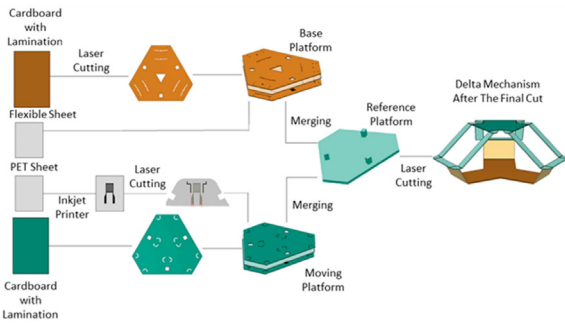


Figure 3. Layer-by-layer fabrication method of Delta mechanism where inkjet printed sensors are embedded.

The fabrication method of the mechanism is presented in Fig. 3, which only uses layer-by-layer 2D fabrication methods. The base and moving platforms are composed of 5 layers: the two cardboards on the top and bottom of the platforms, one flexible sheet in the middle, and two adhesive layers on the top and bottom cardboard layers for fixing the layers. Carboards are used as rigid layers and laminated with an adhesive layer using a lamination machine (Olympia A3). Special design patterns consisting of necessary joint cuts have been designed. And according to these patterns, the base and moving platforms' rigid layers are cut using a laser cutter machine (Aeon Nova 7). Flexible sheets are embedded in the rigid top and bottom layers, which behave as joints on the layer openings. Next, the base and moving platform layers are merged using another adhesive layer on the connection points of the lower arms and the parallelogram. At this step, a reference platform was fabricated using a 3D printer to enable the precise merging of the platforms. At the last step, there is a final cut where the previously partially open connections on the platforms are exposed, and fabrication is completed.

As a result, a new origami-based Delta mechanism is designed with fully 2D fabrication methods. The design requires no additional assembly steps other than the basic cut-paste-repeat cycle. The mechanism has a fixed working area of $20 \times 20 \times 20 \text{ mm}^3$, with minimal undesired non-parallel movements. In addition, the kinematic equations and analyzes of the traditional Delta mechanism can be used without any changes. The final Delta mechanism produced is shown in Fig. 4.

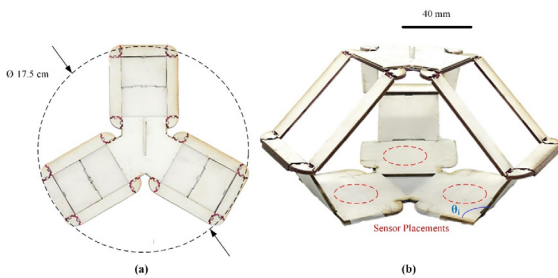


Figure 4. The completed origami-based Delta mechanism (a) folded and (b) opened. The sensors are integrated between rigid layers of the base platform.

Sensor Design, Fabrication, and Integration

The mechanism is produced using the layer-by-layer fabrication method. The flexible layer between the open cuts on the rigid top and bottom layers can bend freely. It provides relative movement between the two parts and connects the two layers. On the other hand, at the bending point of the flexible joints, elongation and shortening occur on the top and bottom surfaces, and accordingly, tensile and compressive stresses occur. Since the flexible layer is pasted between the rigid layers, these stresses depend on the angle between the two parts. The angle between the parts (θ_1 shown in Fig. 4b) can be determined using these stresses.

A sensor layer design has been carried out to sense the stresses on the flexible material between the layers. The strain gauges realize the elongation caused by these effects. As a result, these sensors are printed on PET sheets with silver nanoparticle inks. When the lower arms are actuated, there is a strain on the flexible sensor layer. Due to the strain, there is a resistance change on the printed strain gauges. This resistance change can measure the lower arms' angular position.

The most critical factors in strain gauge design are: leg length, l_{sg} , leg thickness, t_{sg} , number of legs, n_{sg} , and the distance between the legs, d_{sg} (Fig. 5a). The number of legs can be adjusted according to the thickness of the mechanism desired to be produced. The leg length and number generally determine the stationary resistance values of the sensors. l_{sg} and w_{sg} were selected as 18 mm and 14.5 mm, respectively. The distance between the legs and the leg thickness depends on the printer's print quality. Printing a lower resolution than the printer's resolution is impossible. The distance between the legs was determined in such a way that there was no leg contact during the movement. And the leg's thickness was determined, so there was no discontinuity and disconnection between the legs during pressing. Thus, it was decided that the leg thickness, t_{sg} , and spacing between the legs, d_{sg} , would be 0.5 mm. Lastly, the electrode length, l_b , and width, w_b were selected as 11.5 mm and 3.5 mm respectively, again considering the mechanism's geometry.

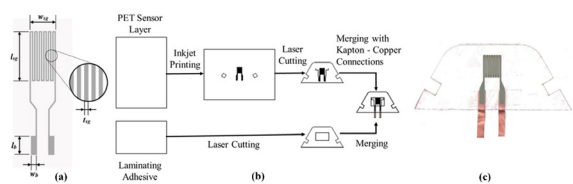


Figure 5. (a) Schematic representation of a strain gauge with important parameters, (b) Fabrication method of an inkjet printed strain gauge, (c) Fabricated sensor.

As can be seen in Fig. 5b, the sensors were realized by printing silver nanoparticle ink (Novacentrix-metalon JS-B25P) on a special PET paper (Novacentrix - Novelle Printing Media) pre-treated for ink retention using an ink-jet printer (Epson L382). Since the printed sensors will take place as a layer in the mechanism, the reference holes used for merging the layers and the isolation sections of the sensor were cut with a laser cutting machine. Thin plastic films are placed in the active working areas of the base platform before placing the sensors in their respective areas. Then, the connection is made with copper-Kapton films to make the wiring from the output electrodes of the sensor. Finally, the cable connection integration is made to the flexible layer with sensors, ready to be placed on the rigid layers.

Since the produced sensor is required to measure the deformation caused by the angle change, the placement of the sensor on the joint is very important. At first, the sensor layer was placed on top of the rigid layers, which is on the joint cut, being in contact with both arms, as seen in Fig. 6a. However, during the movement of the arms, the contact is lost due to the cracks on the silver ink causing to be dysfunctional. The second placement option of the sensor was just below the joint cut, as shown in Fig 6b. As a result, the sensor was in contact with only one arm. Thus, the problem encountered in the previous settlement was eliminated.

A finite element model (FEM) was realized to analyze the strain distribution on the flexible sensor layer during motion. Therefore, a foldable 1 DoF joint composed of rigid and flexible layers was used for the analysis. Three regions of the flexible layer have been examined for sensor placement, as shown in Fig. 7a. In region B, the sensor's PET material experiences major deflections. Whereas in regions A and C, there are minor deflections. Region C belongs to the lower arm and moves when the mechanism is actuated. And this will cause distortions in the output signals of the sensor. That's why this option is eliminated. Fig. 7b shows the analysis realized for the fixed-fixed supported flexible sensor layer. In region A, the strains are in 2 % orders, whereas in region B, the strains are in 30 % orders. So we can conclude that, in region A, the strains are approximately an

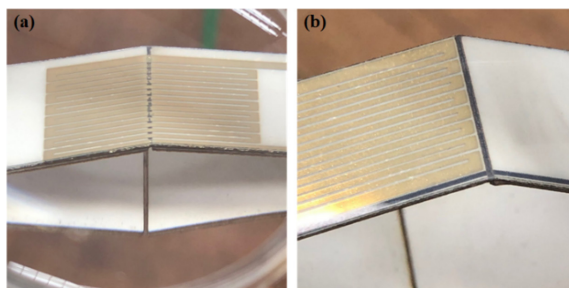


Figure 6. Placement of sensors on the layer. (a) Placing the sensor symmetrically on the movable arms above the joint, (b) Placing the sensor close to the joint on one active arm.

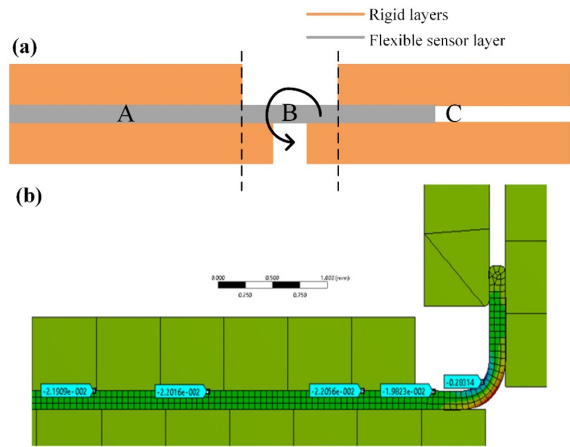


Figure 7. (a) Layers and regions of a foldable joint. Middle layer is the flexible sensor layer, top and bottom layers are the rigid layers, (b) Strain distributions at region A and B for fixed-fixed supported flexible layer.

order below those in region B. So, placing the sensors more on region A will cause fewer strains, preventing cracks on the silver ink that will cause dysfunctions.

Lastly, apart from the settlement location, the sensor was embedded in the top and bottom rigid layers as the flexible layer. As a result, it was seen that embedding the sensor gives better results than placing the sensor on top of the rigid layer. Therefore, the sensors placed on the flexible layer and located just below the reference axis shown in Fig 8b was determined as the sensor's location. Since the Delta mechanism has three separate active lower arms actuated with motors, three sensors are placed independently (Fig 8a). Each sensor has been fabricated separately and used as the flexible layer between the base platform's rigid layers.

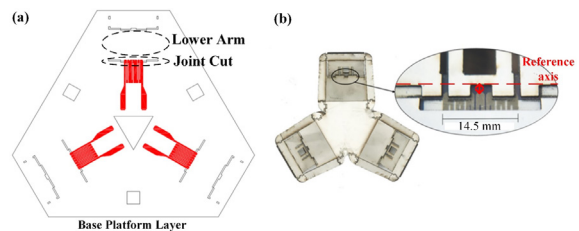


Figure 8. (a) Sensor placement between base platform rigid layers as a flexible layer, (b) Fabricated mechanism with placed printed strain sensors.

Experimental Setup

An experimental setup was developed to actuate the Delta mechanism and analyze the printed sensor outputs (Fig. 9). The mechanism was actuated using servo motors (Dynamixel XL430-W250-t). The moving platform's center motion was recorded using a magnetic-based sensor, Polhemus' Patriot micro sensor, placed at the center of the moving platform. The position sensor reference was fixed on the testing platform, and the position was measured in 6 DoF. The sensors' resistance changes were measured using a Wheatstone bridge circuit which converts

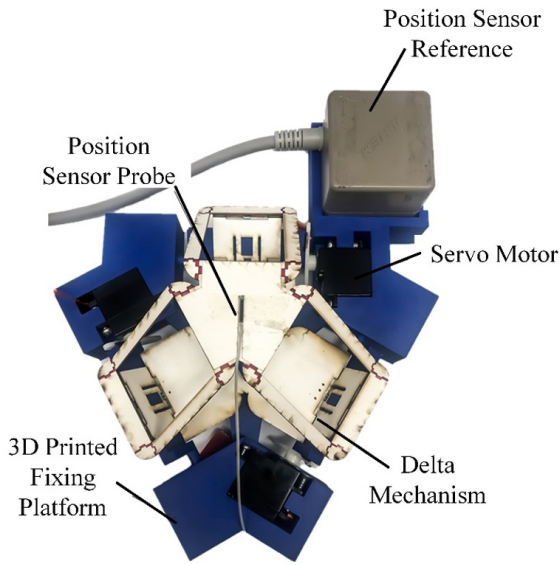


Figure 9. The experimental setup consisting of position sensor, servo motors and servo motors placed on the 3D printed fixing platform.

the resistance changes into voltage outputs. The signals received from the circuit were collected using a data acquisition card (National Instruments USB-6003).

RESULTS AND DISCUSSION

The sensors' output voltages were analyzed using the experimental setup. One of the most critical factors affecting the sensors' voltage output is how high the sensor rises from the axis of rotation. Fig. 10 shows the placement

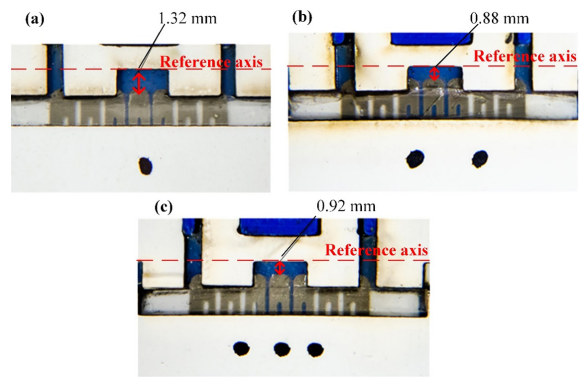


Figure 10. The placement of three sensors embedded in the mechanism named (a) Sensor #1, (b) Sensor #2, and (c) Sensor #3.

of the three sensors where the experiments were carried out. Each sensor has been placed at different distances from the specified reference axis.

Firstly, the active lower arms of the mechanism were actuated by giving a certain angle as a step input and then returning to the original position. Fig. 11a shows the results of 3 sensors. The best results are seen with Sensor #1's voltage output which follows the joint movement. Sensors #2 and #3 returned to a different initial position as the joint returned. These data indicate that there is a hysteresis within the sensor. Then four rising step inputs between 0° and 90° were given to the lower arms. Each incremental step has an amplitude of 22.5° and 3 seconds intervals. Fig. 11b shows the sensors' results of this test. The best tracking was again observed in Sensor #1. In addition, the non-linear structure

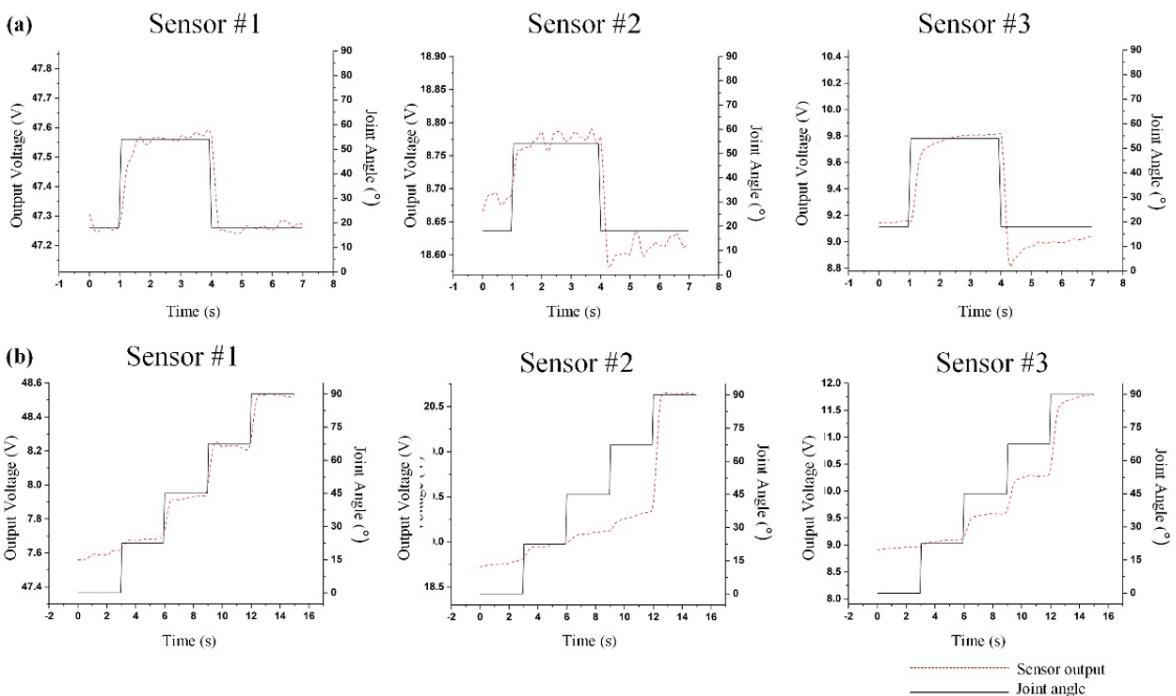


Figure 11. Sensor voltage outputs respect to the joint angle movement: (a) by applying a step input at an angle of 30° for 3 seconds, and (b) by applying four step inputs of 22.5° between 0° and 90° at 3 second intervals to each lower arm.

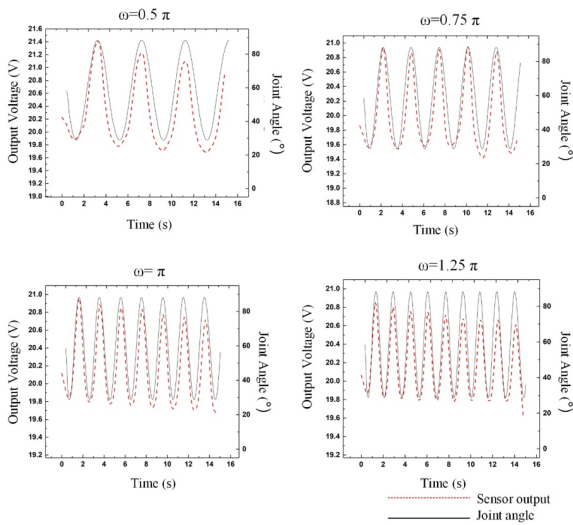


Figure 12. Voltage response of Sensor #1 when the corresponding active joint is driven with sinusoidal inputs with different frequencies.

of the sensor can be seen with this test. While the sensor detects angle changes with lower voltage changes at near zero angles, voltage differences increase at angles close to 90°. This experiment also gives us information about the lowest angle value at which the sensor should work. According to the results, the sensor responds after 20° of joint movement.

After the step input tests, the outputs of the sensors were investigated when sinusoidal motions with different frequencies and different amplitudes were given as inputs for each lower arm. First, sine waves at four different frequencies for 15 seconds were given to the joints. Fig. 12 shows the behavior of Sensor #1. As can be seen, it can follow joint angle movements. However, the hysteresis seems to increase with the increase in frequency.

As seen in the previous tests (Fig. 11), the sensitivity of Sensor #2 is less than that of Sensor #1. However, the change

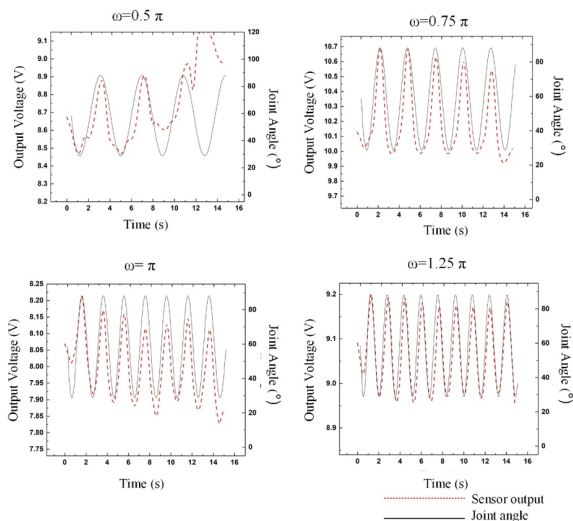


Figure 13. Voltage response of Sensor #2 when the corresponding active joint is driven with sinusoidal inputs with different frequencies.

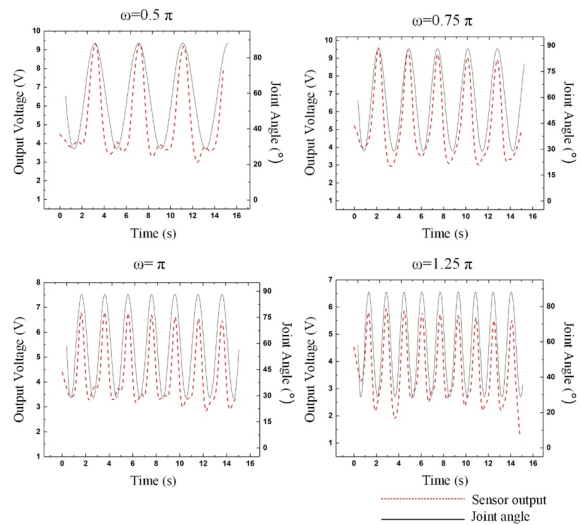


Figure 14. Voltage response of Sensor #3 when the corresponding active joint is driven with sinusoidal inputs with different frequencies.

in frequency affected the behavior of the sensor more, as shown in Fig. 13. At low frequencies, the sensor voltage outputs have meaningless behavior during its movement from 30° to 90°. On the other hand, with the increase in frequency, it can be understood that it follows the same movement more clearly. It was observed that the sensors showed better behavior when the frequency was 0.75 π .

The sensitivity of Sensor #3 is higher than that of Sensor #2. However, unpredictable behaviors emerged at different frequencies. This unexpected behavior around 30° can be seen in Fig. 14. This indefinite motion decreased with increasing frequency, but increasing frequency caused an increase in hysteresis.

After the frequency experiments, it was also analyzed how the sensors responded at three different amplitudes (30°-50°, 30°-70°, 30°-90°) of sinusoidal inputs. According to the frequency test results, the frequency of the sine wave was chosen as 0.75 π . Sensor #1 gave the best result and showed similar behavior at three different amplitudes (Fig. 15a). However, Sensor #2 can not follow the angular motion as well as Sensor #1 and #3 (Fig. 15b). Better results were obtained with large amplitude compared to lower amplitudes. Finally, similar behavior was observed in Sensor #3 (Fig. 15c). Again, better results and input profile tracking were seen at large amplitude. In addition, it showed less hysteresis behavior between 30°-70° compared to Sensor #2.

The final test is the simultaneous comparison of the fabricated sensors, the position sensor placed on the center of the moving platform (Fig. 9). A circle with a diameter of 10 mm is given to the movable platform as input. According to the kinematic model, the lower arms draw a sine wave with different phase angles. The joint angles are calculated using the measurements from the position sensor and inver-

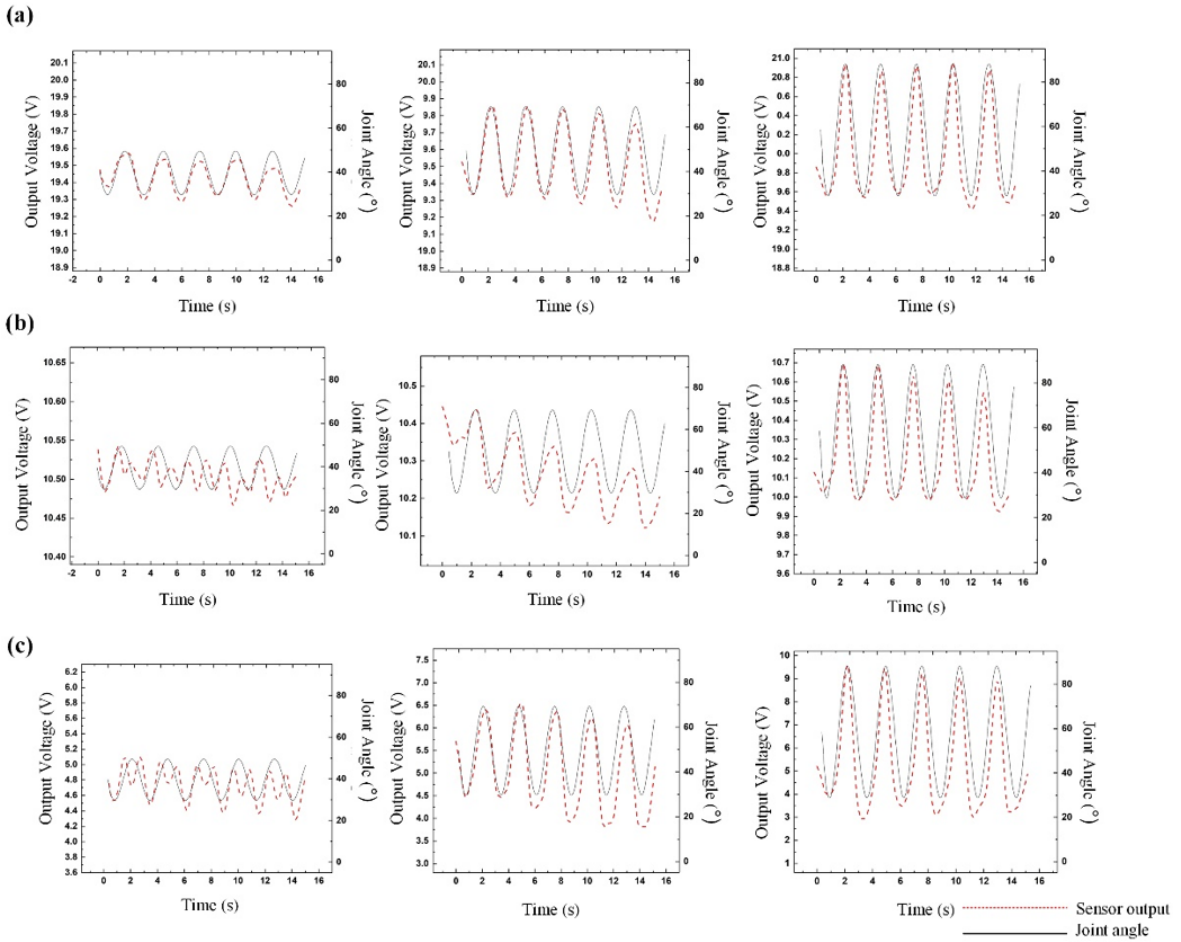


Figure 15. The voltage responses of Sensor #1 (a), Sensor #2 (b), and Sensor #3 (c) when the corresponding active joint is driven with sinusoidal inputs with different amplitudes.

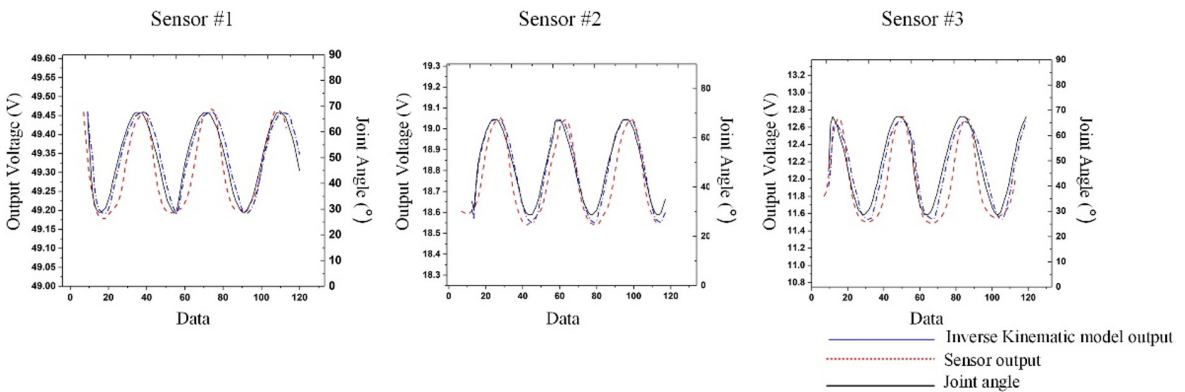


Figure 16. The comparison of fabricated sensors, position sensor, and kinematic model when the moving platform's center draws a circle of 10 mm.

se kinematic model. When the results are examined, shown in Fig. 16, it is seen that the data of the position sensor and the manufactured sensor follow the data of the kinematic model. This result shows that the integrated inkjet printed sensors can be used as a direct measurement for the active joints and for controlling the mechanism.

CONCLUSION

Design and fabrication of scalable, customizable, low profile and foldable robots is very popular in robotics science because of varied applications requiring smaller scale mechanisms. It is also important to find easy and low-cost solutions for this purpose. The production of

the mechanisms' structure is needed. However, to monitor and control the motion of these mechanisms, sensor integration is essential. This paper presents a novel origami-based Delta mechanism's position sensor integration. Predefined strain gauge patterns were printed on the PET sheet using Ag NP inks with desktop printers, and a flexible sensor layer was created. The placement of the sensors as a flexible layer of the mechanism was studied by giving step and sinusoidal inputs to the active lower arms. The resistance changes of the sensors have been converted to voltage outputs. The sensors' voltage responses have been collected to see if the sensor can track the angle position during the motion. The results show that the presented methodology for position sensing gives promising results for providing angular position feedback to a position control loop. The critical findings from this work can be summarized as follows:

- It has been found that the strain gauge sensors should be inside the rigid layers because when the arms of the mechanism are actuated, there are tension and compression stresses between the layers. This causes strain on the sensor related to the motion of the arms.

- The location of the sensors affects the signals. The best results were realized with the sensor close to the joint cuts' rotation axis.

- It has been shown that functional layers can be embedded in an origami-based structure, making the mechanism more customizable, low-profile, and compact.

For future work, the strain sensors will be placed in the determined location gathered from this work. And the mechanism's position control will be performed using these integrated sensors, which can significantly contribute to the origami-based mechanisms' literature. Besides, this methodology can be applied to other parallel mechanisms and used in defined applications.

ACKNOWLEDGMENT

This work was supported by the Scientific and Technological Research Council of Turkey (TÜBİTAK), Grant No: 216M193.

CONFLICT OF INTEREST

Authors approve that to the best of their knowledge, there is not any conflict of interest or common interest with an institution/organization or a person that may affect the review process of the paper.

References

1. López M, Castillo E, García G, Bashir A. Delta robot: Inverse, direct, and intermediate Jacobians. *Proceedings of the Institution of Mechanical Engineers Part C: Journal of Mechanical Engineering Science* 220 (2006) 103-109.
2. Vischer P, Clavel R, Argos A. Novel 3-DoF Parallel Wrist Mechanism. *The International Journal of Robotics Research* 19 (2000) 5-11.
3. Rey L, Clavel R. The Delta Parallel Robot. *Parallel Kinematic Machines* 53 (1999) 401-417.
4. Pernette E, Henein S, Magnani I, Clavel R. Design of parallel robots in microrobotics. *Robotica* 15 (1997) 417-420.
5. Codourey A, Perroud S, Mussard Y. Miniature Reconfigurable Assembly Line for Small Products, in: Ratchev S (Eds.). *Precision Assembly Technologies for Mini and Micro Products*. Paper presented at IPAS 2006, Bad Hofgastein, 19-21 February. Springer, Boston, pp. 193-200, 2006.
6. Tanikawa T, Ukiana M, Morita K, Koseki Y, Ohba K, Fujii K, Arai T. Design of 3DOF Parallel Mechanism with Thin Plate for Micro Finger Module in Micro Manipulation. Paper presented at IEEE/RSJ International Conference on Intelligent Robots and Systems, EPFL, Lausanne, 30 September-04 October. IEEE, pp. 1778-1783, 2002.
7. Whitney JP, Sreetharan PS, Ma KY, Wood RJ. Pop-up book MEMS. *Journal of Micromechanics and Microengineering* 21 (2011) 115021-115027.
8. Wood RJ. Design, fabrication, and analysis of a 3DOF, 3cm flapping-wing MAV. Paper presented at IEEE/RSJ International Conference on Intelligent Robots and Systems, San Diego, 29 October-2 November. IEEE, pp. 1576-1581, 2007.
9. Birkmeyer P, Peterson K, Fearing RS. DASH: A dynamic 16g hexapedal robot. Paper presented at IEEE/RSJ International Conference on Intelligent Robots and Systems, St. Louis, 10-15 October. IEEE, pp. 2683-2689, 2009.
10. Baisch AT, Ozcan O, Goldberg B, Ithier D, Wood RJ. High speed locomotion for a quadrupedal microrobot. *The International Journal of Robotics Research* 33 (2014) 1063-1082.
11. Zhakypov Z, Mori K, Hosoda K, Paik J. Designing minimal and scalable insect-inspired multi-locomotion millirobots. *Nature* 571 (2019) 381-386.
12. Jafferis NT, Helbling EF, Karpelson M, Wood RJ. Untethered flight of an insect-sized flapping-wing microscale aerial vehicle. *Nature* 570 (2019) 491-495.
13. Russo S, Ranzani T, Gafford J, Walsh CJ and Wood RJ. Soft pop-up mechanisms for micro surgical tools: Design and characterization of compliant millimeter-scale articulated structures. Paper presented at IEEE International Conference on Robotics and Automation, Stockholm, 16-21 May. IEEE, pp. 750-757, 2016.
14. Gafford J, Ranzani T, Russo S, Aihara H, Thompson C, Wood R, Walsh C. Snap-On Robotic Wrist Module for Enhanced Dexterity in Endoscopic Surgery. Paper presented at IEEE International Conference on Robotics and Automation, Stockholm, 16-21 May. IEEE, pp. 4398-4405, 2016.
15. Salerno M, Zhang K, Mencias A and Dai JS. A novel 4-DOFs origami enabled, SMA actuated, robotic end-effector for minimally invasive surgery. Paper presented at IEEE International Conference on Robotics and Automation (ICRA), Hong Kong, 31 May-7 June. IEEE, pp. 2844-2849,

- 2014.
16. Temel FZ, McClintock H, Doshi N, Koh JS, and Wood RJ. The MilliDelta: A High-Bandwidth, High-Precision, Millimeter-Scale Delta Robot. *Science Robotics* 3 (2018) eaar3018.
17. Mintchev S, Salerno M, Cherpillod A, Scaduto S, Paik J. A portable three-degrees-of-freedom force feedback origami robot for human-robot interactions. *Nature Machine Intelligence* 1 (2019) 584-593.
18. Kalafat MA, Sevinç H, Samankan S, Altınkaynak A, and Temel Z. A Novel Origami-Inspired Delta Mechanism With Flat Parallelogram Joints. *ASME Journal of Mechanisms and Robotics* 13 (2021) 021005.
19. Firouzeh A, Amon-Junior AF, Paik J. Soft piezoresistive sensor model and characterization with varying design parameters. *Sensors and Actuators A: Physical* 233 (2015) 158-168.
20. Kwak B, Bae J. Compliant mechanosensory composite (CMC): a compliant mechanism with an embedded sensing ability based on electric contact resistance. *Smart Materials and Structures* 27 (2018) 125003.
21. Maddipatla D, Narakathu BB, Atashbar M. Recent Progress in Manufacturing Techniques of Printed and Flexible Sensors: A Review. *Biosensors* 10 (2020) 199.
22. Ando B, Baglio S. All-inkjet printed strain sensors. *IEEE Sensors Journal* 13 (2013) 4874-4879.
23. Sun X, Felton SM, Wood RJ, Kim S. Printing angle sensors for foldable robots. Paper presented at IEEE/RSJ International Conference on Intelligent Robots and Systems (IROS), Hamburg, 28 September-2 October. IEEE, pp. 1725-1731, 2015.
24. Vadgama N, Steimle J. Flexy: Shape-customizable, single-layer, inkjet printable patterns for 1D and 2D flex sensing. Paper presented at Eleventh International Conference on Tangible, Embedded, and Embodied Interaction, Yokohama, 20-23 March. Association for Computing Machinery, New York pp.153-162, 2017.
25. Ando B, Baglio S, Bulsara AR, Emery T, Marletta V, Pistorio A. Low-Cost Inkjet Printing Technology for the Rapid Prototyping of Transducers. *Sensors* 17 (2017) 748.
26. Correa JE, Toombs J, Toombs N, Ferreira PM. Laminated Micro-Machine: Design and Fabrication of a Flexure-Based Delta Robot. *Journal of Manufacturing Processes* 24 (2016) 370-375.